

Urolithin as a Converging Scaffold Linking Ellagic acid and Coumarin Analogues: Design of Potent Protein Kinase CK2 Inhibitors

Giorgio Cozza,^[a] Alessandra Gianoncelli,^[a] Paolo Bonvini,^[b, c] Elisa Zorzi,^[c] Riccardo Pasquale,^[d] Angelo Rosolen,^[b] Lorenzo A. Pinna,^[a] Flavio Meggio,^[a] Giuseppe Zagotto,^[d] and Stefano Moro^{*[d]}

Casein kinase 2 (CK2) is a ubiquitous, essential, and highly pleiotropic protein kinase; its abnormally high constitutive activity is suspected to underlie its pathogenic potential in neoplasia and other relevant diseases. Previously, using different *in silico* screening approaches, two potent and selective CK2 inhibitors were identified by our group: ellagic acid, a naturally occurring tannic acid derivative ($K_i = 20$ nM) and 3,8-dibromo-7-hydroxy-4-methylchromen-2-one (DBC, $K_i = 60$ nM). Comparing the crystallographic binding modes of both ellagic acid and DBC, an X-ray structure-driven merging approach was taken to design

novel CK2 inhibitors with improved target affinity. A urolithin moiety is proposed as a possible bridging scaffold between the two known CK2 inhibitors, ellagic acid and DBC. Optimization of urolithin A as the bridging moiety led to the identification of 4-bromo-3,8-dihydroxy-benzo[*c*]chromen-6-one as a novel, potent and selective CK2 inhibitor, which shows a K_i value of 7 nM against the protein kinase, representing a significant improvement in affinity for the target compared with the two parent fragments.

Introduction

Casein kinase 2 (CK2) is probably the most pleiotropic protein kinase known, with more than 300 protein substrates already recognized—a feature that might, at least partly, account for its lack of strict control over catalytic activity.^[1,2] Its catalytic subunits (α and/or α') are constitutively active either with or without the regulatory β -subunits, which appear to play a role in targeting and substrate recruiting, rather than controlling catalytic activity. Furthermore, constitutively active CK2 is ubiquitous, essential, and implicated in a wide variety of important cell functions.^[3] Evidence has been accumulating that the catalytic subunits of CK2 behave as oncoproteins,^[4–7] consistent with the observation that they display an antiapoptotic effect in prostate cancer cells.^[8] CK2 subunits are more abundant in tumors as compared with normal tissues, and their overexpression is causative of neoplastic growth in animal and cellular models, giving rise to alterations in the expression levels of cellular oncogenes or tumor suppressor genes.^[9] These data, in conjunction with the observation that many viruses exploit CK2 as a phosphorylating agent of proteins essential to their life cycle,^[1] are raising interest in CK2 as a potential target for antineoplastic and/or anti-infectious agents.^[10] CK2 has also been implicated in glomerulonephritis,^[11] a progressive kidney inflammation that is the primary cause of chronic renal failure and end-stage renal disease, and is known to play a critical role in the progression of immunogenic renal injury,^[11] making CK2 a promising potential target for therapy in renal diseases.

In recent years, our group has undertaken an intensive screening program, using both conventional and *in silico* approaches, with the aim of discovering novel, potent and selec-

tive CK2 inhibitors.^[12,13] In this context, several new derivatives have been reported as potent and selective CK2 inhibitors, such as ellagic acid (1),^[14] a naturally occurring tannic acid derivative, 3,3',4',7-tetra-hydroxyflavone (fisetin),^[15] tetrabromocinnamic acid (TBCA),^[16] 1,2,5,8-tetrahydroxy-antraquinone (quinalizarin),^[17] 1,8-dihydroxy-4-nitroxanthene-9-one (MNX),^[13] 8-hydroxy-4-methyl-9-nitrobenzo[*g*]chromen-2-one (NBC),^[12] 3,8-dibromo-7-hydroxy-4-methylchromen-2-one (DBC),^[13] and 2,7-dihydroxy-3,6-dinitro-fluoren-9-one (FL12),^[13] as summarized in Figure 1.

Recently, the crystallographic structures of both ellagic acid and DBC in complex with the α -subunit of CK2 have been deposited into the Protein Data Bank (PDB) with the entry codes: 2ZJW and 2QC6, respectively.^[18,19] The availability of structural information is generally accepted to be a requirement for the

[a] Dr. G. Cozza, Dr. A. Gianoncelli, Prof. Dr. L. A. Pinna, Prof. Dr. F. Meggio
Department of Biological Chemistry, University of Padova
Viale Giuseppe Colombo 3, 35131 Padova (Italy)

[b] Dr. P. Bonvini, Prof. A. Rosolen
Clinica di Oncoematologia Pediatrica, Azienda Ospedaliera
University of Padova, Via Giustiniani 3, 35128 Padova (Italy)

[c] Dr. P. Bonvini, Dr. E. Zorzi
Fondazione Città della Speranza
Viale del Lavoro 12, 36034 Monte di Malo, Vicenza (Italy)

[d] Dr. R. Pasquale, Prof. Dr. G. Zagotto, Prof. Dr. S. Moro
Molecular Modeling Section (MMS), Dipartimento di Scienze Farmaceutiche
Università di Padova, via Marzolo 5, Padova (Italy)
stefano.moro @unipd.it

Supporting information for this article is available on the WWW under <http://dx.doi.org/10.1002/cmdc.201100338>.

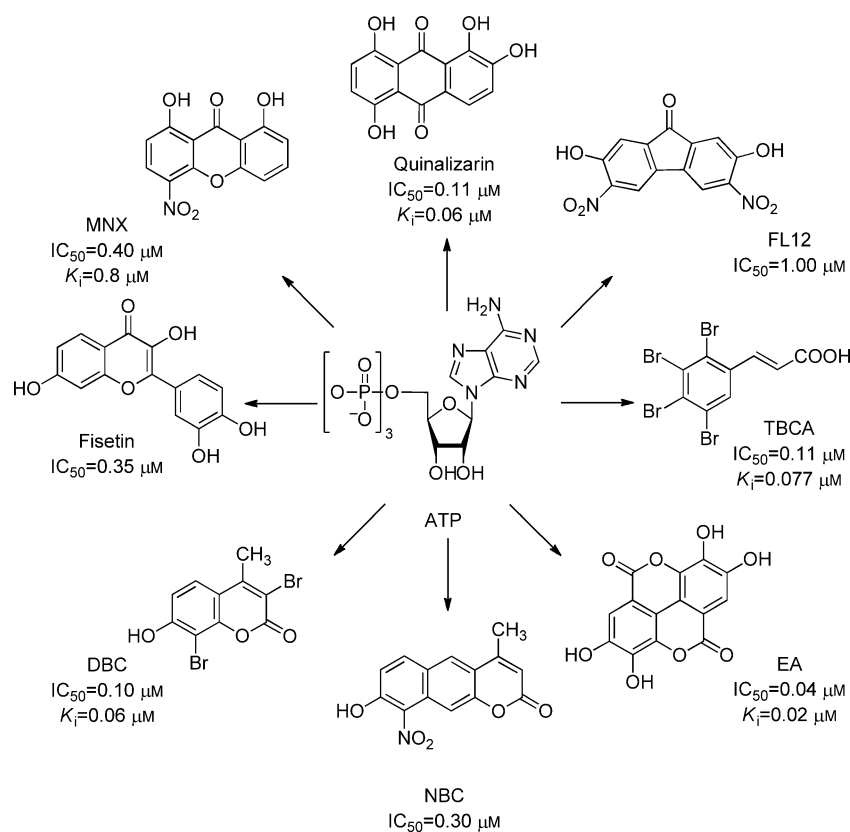


Figure 1. Chemical structures of known CK2 inhibitors and their biological activities against CK2 taken from the literature.^[12–17]

rational design of novel inhibitors using structure-based ligand design approaches. Among these, we decided to apply an X-ray structure-driven merging approach to design novel CK2 inhibitors. In particular, comparing the crystallographic binding modes of both ellagic acid and DBC, we suggest urolithin as a suitable converging scaffold linking ellagic acid and coumarin analogues (Figure 2).

In the present work, we synthesized and tested a focused library of urolithin derivatives with the aim of elucidating their putative binding motifs and possible structure–activity relationships. Optimization of urolithin A led to the identification of a potent and selective derivative, 4-bromo-3,8-dihydroxy-benzo[*c*]-chromen-6-one (**21**), with a K_i value of 7 nM against CK2.

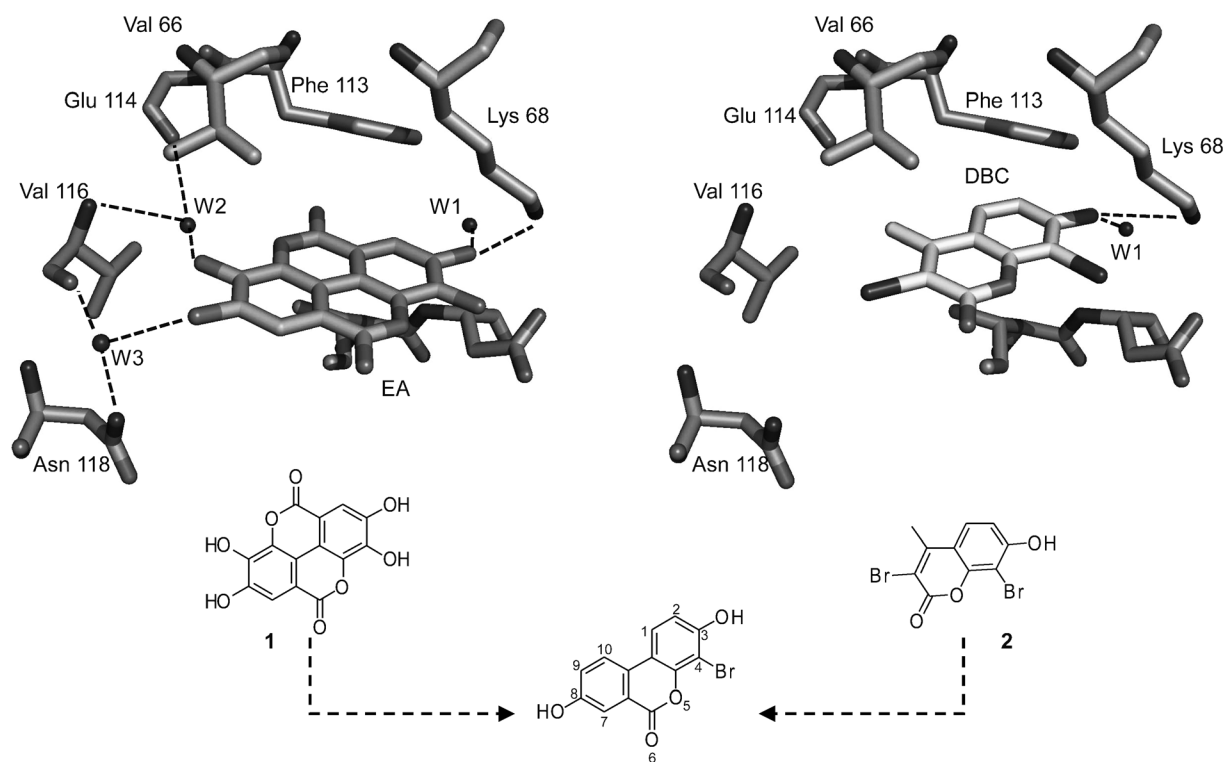


Figure 2. Overview of our structural merging approach, combining the features of both compounds **1** and **2** to create a high-affinity inhibitor.

Results and Discussion

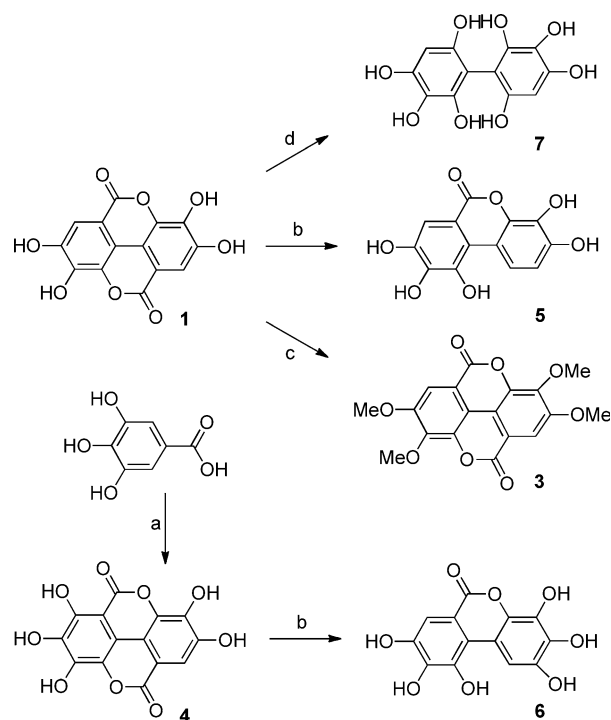
As previously mentioned, the crystallographic structures of the α -subunit of CK2 in complex with both ellagic acid (PDB: 2ZJW) and DBC (PDB: 2QC6) have recently been described.^[18,19] Like all known inhibitors of CK2, where the α -subunit crystal structure is available, both ellagic acid and DBC bind inside the ATP binding cleft of the catalytic domain of CK2, and they can be classified as type I or ATP-competitive inhibitors.

As shown in Figure 2, ellagic acid and DBC interact with Lys68 through a water-mediated hydrogen bond with the phenolic group at positions 3 and 7 of ellagic acid and DBC, respectively. This water molecule (W1) is highly conserved in all available crystallographic structures, suggesting its fundamental role in maintaining the correct conformational features of the CK2 catalytic site.^[19]

However, while DBC does not bind the hinge region directly, ellagic acid interacts both with the hinge region and the ATP phosphate group binding area, as deduced by the three-dimensional crystallographic complex recently reported.^[18] The hydroxy group at position 7 of ellagic acid interacts with the carboxyl oxygen of the hinge-region residue Glu 114 through a water bridge (W2), while the hydroxy group in position 8 binds a nearby water molecule (W3) connected to Asn 118 and a carboxyl oxygen of Val 116 in the hinge region. On the other side, the hydroxy groups at positions 3 and 2 interact with the side chains of Lys 68 and Asp 175, respectively.^[18]

Furthermore, the hydroxy group at position 7 of the coumarin moiety has already been described as an essential feature for activity, even though it alone is not sufficient to achieve an IC_{50} value in the sub-micromolar range.^[19] Indeed, to increase the inhibitory potency, an electron-withdrawing substituent should be simultaneously present at position 8. As expected, an electron-withdrawing substituent *ortho* to a phenol group increases the pK_a of the phenol, reinforcing the robustness of the crucial water-mediated hydrogen bond. This hypothesis is also supported by the fact that substitution of the 7-hydroxy group in DBC with a 7-amine or 7-methoxy group results in a complete loss of activity.^[19] With the aim to expand the structure–activity relationships known for ellagic acid (1) with CK2, we demonstrate that both methylation of all hydroxy groups (compound 3) and the introduction of an additional hydroxy at position 1 (flavellagic acid, 4) drastically reduce the affinity of both analogues for CK2 (Table 1).

In addition, hydrolysis under mild basic conditions of both ellagic (1) and flavellagic (4) acids provides derivatives 5 and 6, respectively (Scheme 1; complete details of the synthesis are given in the Experimental Section). Both analogues 5 and 6 belong to the so-called hydrolysable tannins or urolithins, and they show interesting binding affinities to CK2 (IC_{50} = 0.20 μ M and 2.20 μ M, respectively; Table 1). Indeed, as already observed with the precursors, derivative 5 is one order of magnitude more active than 6, supporting the concept that the introduction of an additional hydroxy group is detrimental to the binding affinity of ellagic acid analogues. Finally, hydrolysis of ellagic acid (1) conducted under much stronger conditions gives



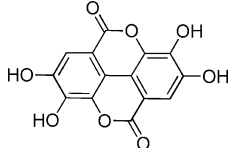
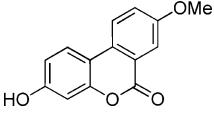
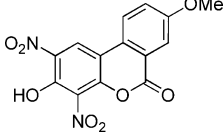
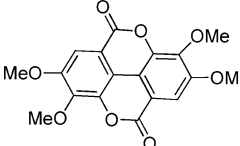
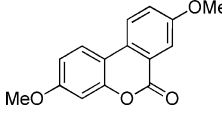
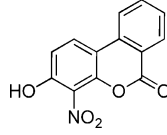
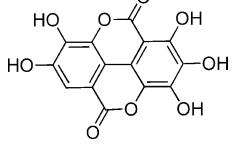
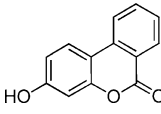
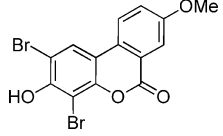
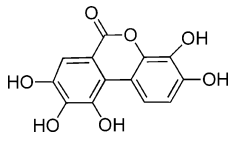
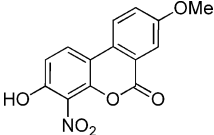
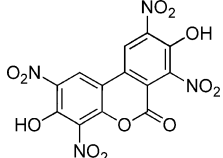
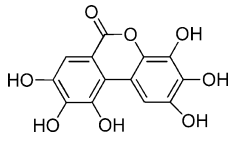
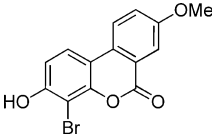
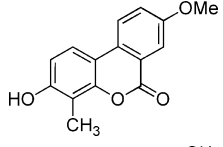
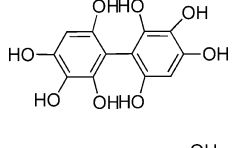
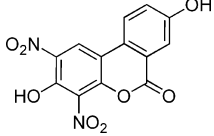
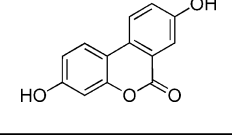
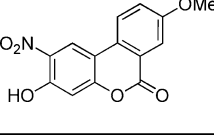
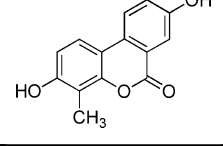
Scheme 1. Reagents and conditions: a) H_2SO_4 (96%), H_2O , $K_2S_2O_8$, 4 °C, overnight; b) KOH, H_2O , reflux, 0.5 h; c) CH_3I , NaH, DMF, 0 °C, 2 h; d) NaOH, 300 °C, 20 min.

poly-hydroxyl-biphenyl analogue 7 that maintains an appreciable binding affinity for CK2 (IC_{50} = 0.36 μ M; Table 1).

These data indicate that the urolithin moiety might be a converging scaffold linking ellagic acid and coumarin analogues. Following these preliminary data, we tested the inhibitory activity of urolithin A (8), a natural metabolite of ellagic acid that exhibits antioxidant behavior and has several potential therapeutic applications.^[20–22] Chemically, urolithin A is structurally related to compound 5, with the two hydroxy groups at positions 3 and 8 maintained. Urolithin A binds to CK2 in the sub-micromolar range (IC_{50} = 0.39 μ M, Table 1), confirming that the hydroxy groups at positions 3 and 8 can be considered key interactors within the CK2 binding cleft. Furthermore, our molecular docking experiments support the hypothesis that ellagic acid and urolithin A share the same binding motif in the CK2 binding cavity, with the two crucial hydrogen-bonding interactions mediated by the two water molecules W1 and W3 preserved (Figure 3). In particular, W1 plays a pivotal role in mediating the interaction between the hydroxy group at position 3 and Lys68.

In fact, methylating the hydroxy group in position 8 to give the methoxy analogue 9 (Scheme 2; complete details of the synthesis are given in the Experimental Section) reduces the inhibitory activity by one order of magnitude (IC_{50} = 3.5 μ M), while the same substitution at both positions 3 and 8 to give the dimethoxy analogue 10 results in a complete loss of activity (IC_{50} > 40 μ M). By comparison, deletion of the hydroxy group at position 8 and while maintaining the hydroxy group at position 3 (11) drastically compromises the inhibitory activity against CK2 (IC_{50} = 6.5 μ M).

Table 1. Inhibition of CK2 by urolithin analogues.

Compd	IC ₅₀ ^[a] [μM]		Compd	IC ₅₀ ^[a] [μM]		Compd	IC ₅₀ ^[a] [μM]				
	nCK2 ^[b]	CK2α ^[c]		nCK2 ^[b]	CK2α ^[c]		nCK2 ^[b]	CK2α ^[c]			
	1	0.04	0.06		9	3.50	-		16	3.0	-
	3	> 40	-		10	> 40	-		17	0.30	-
	4	2.1	2.5		11	6.5	-		18	0.3	-
	5	0.20	-		12	0.026	0.031		19	> 40	-
	6	2.2	-		13	0.015	0.018		20	2.5	2.2
	7	0.36	-		14	0.6	-		21	0.015	0.021
	8	0.39	0.31		15	2.0	-		22	4.2	5.5

[a] IC₅₀ values represent the mean of three independent experiments with the SEM not exceeding 15%. [b] Native CK2 purified from rat liver. [c] Human recombinant α subunits of CK2 (see Experimental Section). Ellagic acid (1), flavellagic acid (4), and urolithin A (8).

Based on these findings, we investigated the effect of electron-withdrawing substituents at position 4 of urolithin A, with the aim to mimic the very beneficial effect already observed for coumarin analogues. Molecular docking simulations predict good structural superposition of the coumarin position 8 in its crystallographic pose and position 4 of urolithin A. It has already been shown that electron-withdrawing substituents, such as nitro or bromo groups, at position 8 of the 7-hydroxy-4-methylchromen-2-one scaffold significantly increase the binding affinity of a compound to CK2.^[19] Here, we confirm that position 4 of urolithin A is compatible, with both nitro (12) or bromo (21) substitutions in this specific position (Figure 4).

After considering the synthetic feasibility of preparing urolithin A derivatives with a nitro- or bromo substituent at posi-

tion 4, we decided to make both 3-hydroxy-8-methoxy-4-nitrobenzo[c]chromen-6-one (12) and 3-hydroxy-8-methoxy-4-bromo-benzo[c]chromen-6-one (13); the corresponding 8-hydroxy analogue (21) was also prepared (Scheme 3; complete details of the synthesis are given in the Experimental Section).

As expected, both derivatives 12 and 13 are potent inhibitors of CK2 activity, with relative IC₅₀ values in the low nanomolar range (IC₅₀ = 26 nM and 15 nM, respectively). As already observed for coumarin analogues, the beneficial role of an electron-withdrawing substituent *ortho* to the phenol group was confirmed. With respect to all other modifications, only the specific combination of the 3-hydroxy and 4-nitro (or 4-bromo) in the 8-methoxy-benzo[c]chromen-6-one scaffold gave compounds with improved CK2 binding affinity (Table 1). In particular, modifications like the presence of an electron-do-

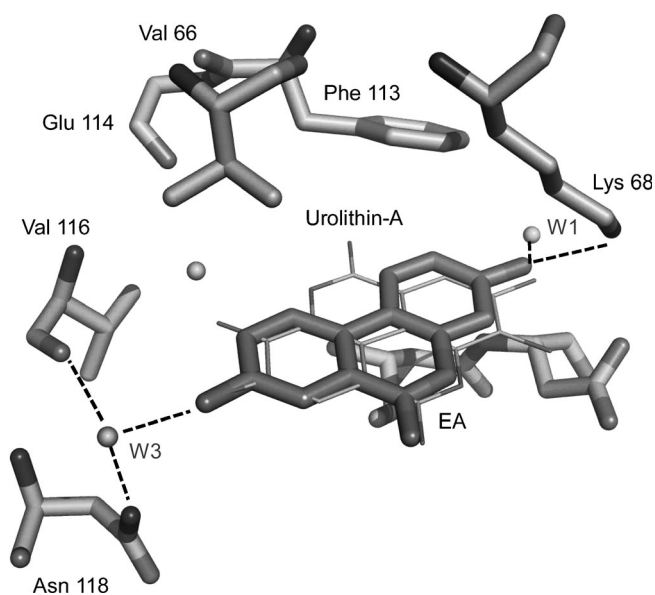
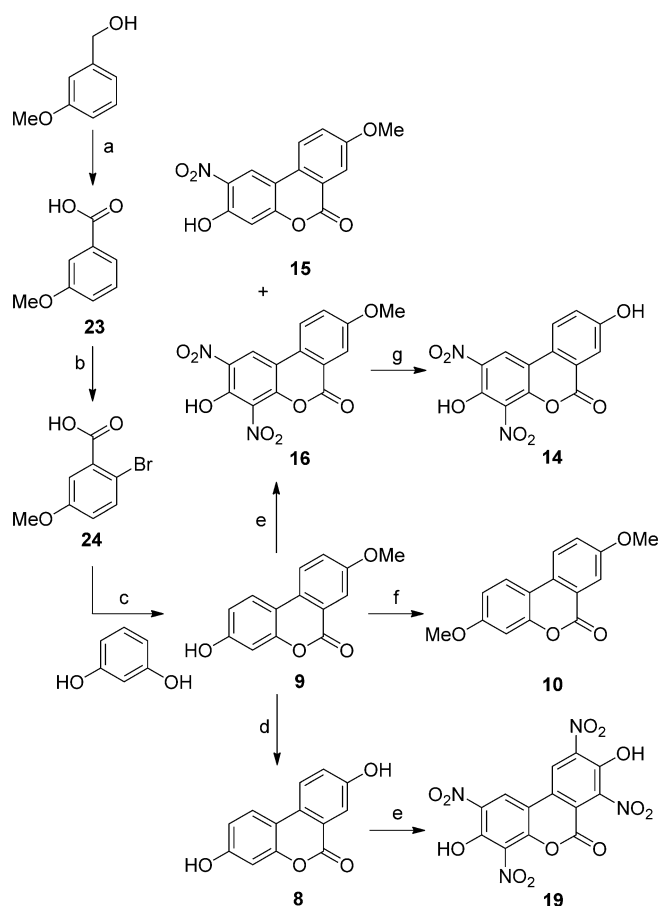


Figure 3. Molecular modeling results for urolithin A (**8**) docked to the active site of human CK2 (PDB: 2ZJW^[18]).



Scheme 2. Reagents and conditions: a) KMnO_4 , NaOH, reflux, 1 h; b) Br_2 , AcOH, reflux, 3 h; c) CuSO_4 , NaOH, reflux, 1 h; d) HBr, AcOH, reflux, 11 h; e) HNO_3 (65%), AcOH, 50 °C, 4 h; f) dimethylsulfate, K_2CO_3 , acetone, reflux, 1 h; g) pyridine-HCl, 210 °C, 4 h.

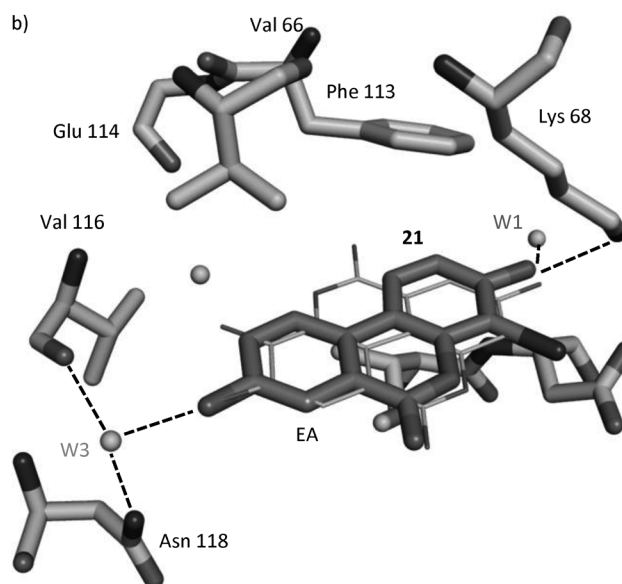
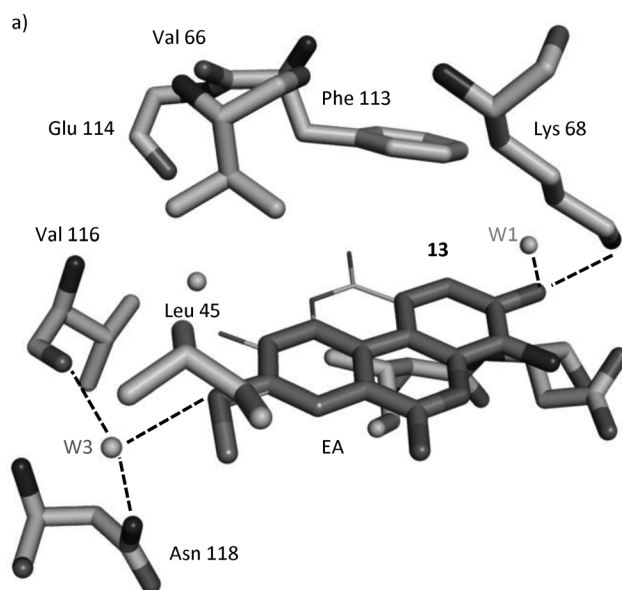


Figure 4. Molecular modeling results for compounds a) **13** and b) **21** docked to the active site of human CK2 (PDB: 2ZJW^[18]).

nating substituent at position 4, such as a methyl group (**20**), or a shift of the electron-withdrawing substituent to position 2 (**15**), were not tolerated.

Supporting our initial hypothesis, hydrolysis of compound **13** gave the corresponding 4-bromo-3,8-dihydroxy-benzo[*c*]chromen-6-one (**21**), which maintained potent ATP-competitive CK2 inhibitory activity ($\text{IC}_{50} = 0.015 \mu\text{M}$), with a K_i value, calculated from linear regression analysis of Lineweaver–Burk double reciprocal plots, closed to $0.007 \mu\text{M}$ which is among the lowest reported so far (Figure 5). Moreover, according to a preliminary selectivity study, compound **21** resulted quite specific for CK2 when tested against a representative panel of kinases (Table 2).

To explore the potential oncological applications of the more promising novel CK2 inhibitors, the cytotoxicity profile of

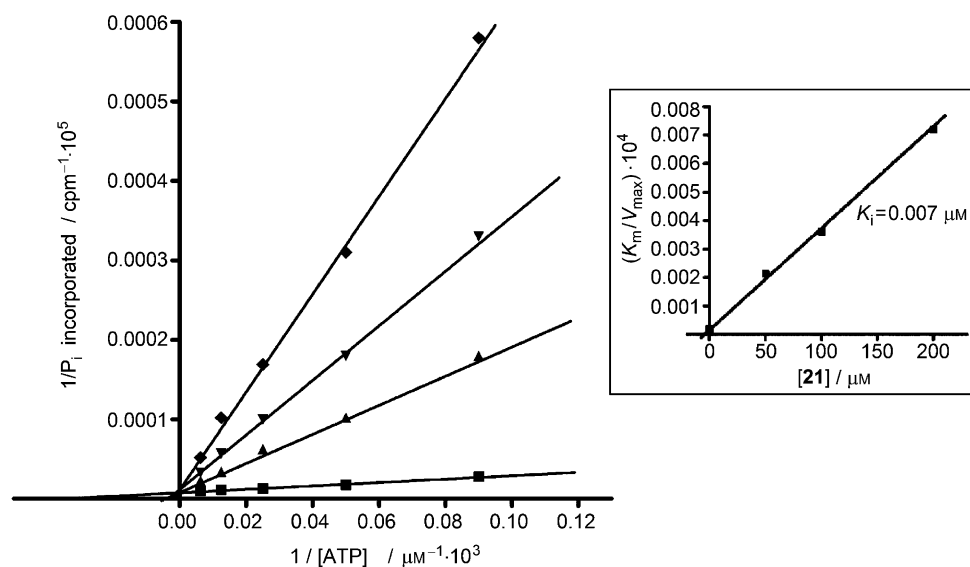


Figure 5. Kinetic analysis of compound 21–CK2 complexation consistent with a reversible and competitive mechanism of inhibition. The inset shows the determination of the K_i value for CK2 inhibition by 21. CK2 activity was determined as described in the Experimental Section either in the absence (■) or presence of compound 21: 200 nM (◆); 100 nM (▼); 60 nM (▲). Data represent the mean of triplicate experiments with the SEM not exceeding 15%.

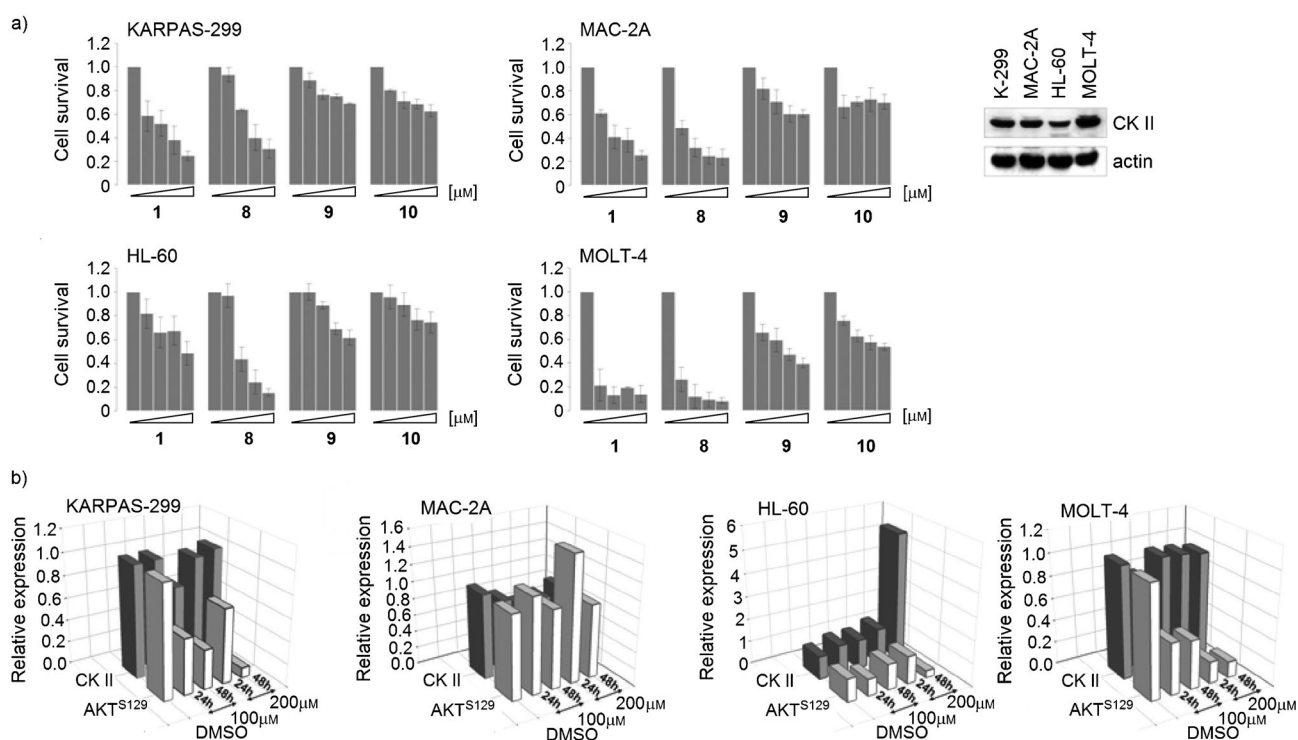


Figure 6. a) Effect of CK2 inhibitors on tumor cell survival. KARPAS-299, MAC-2A, MOLT-4 and HL-60 cell lines were treated with increasing concentrations (50, 100, 150, 200 μM) of ellagic acid (**1**), urolithin A (**8**) and derivatives **9** and **10** as described in the Experimental Section. Cell growth was measured by an MTT assay after 48 h exposure. Data are the mean absorbance of three replicate wells, of three independent experiments, relative to untreated controls (bars \pm SD). Control cells were exposed to DMSO and assigned a viability value of 1.0. CK2 protein expression as assessed by Western blot is also shown (right). b) Dose- and time-dependent analysis of urolithin A (**8**) activity on CK2 expression and activity, performed using antibodies specific for total CK2 and phosphorylated AKT (AKT^{S129}). Exponentially growing cells were treated with 100 and 200 μM of **8** for either 24 h or 48 h, and whole lysates of treated and untreated cells were probed with the indicated antibodies. Relative changes in expression levels of CK2 and phospho-AKT were obtained by densitometric analysis of the corresponding blots, and graphically expressed as fold change over DMSO-treated controls.

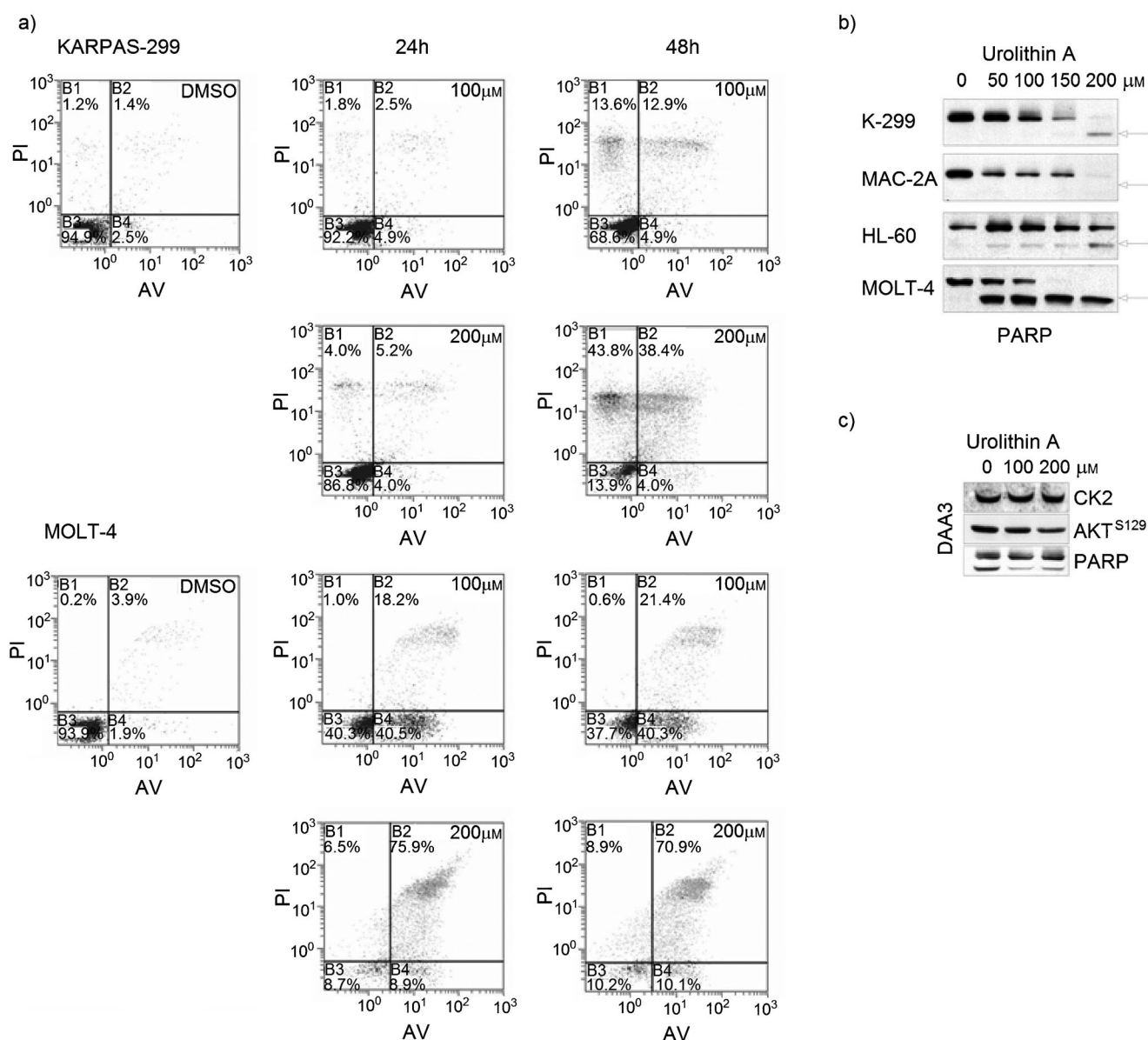


Figure 7. a) Apoptosis induction in tumor cells exposed to urolithin A. Selected concentrations (100 and 200 μM) of urolithin A (**8**) were used to treat KARPAS-299 and MOLT-4 cells for both 24 and 48 h. Urolithin-treated and untreated cells were stained with annexin-V (AV) and propidium iodide (PI) and analyzed using a fluorescence-activated cell sorter (FACS) instrument. Percentages of viable (AV⁻/PI⁻), early apoptotic (AV⁺/PI⁻), late apoptotic (AV⁺/PI⁺) and necrotic cells (AV⁻/PI⁺) are reported in quadrants B3, B4, B2 and B1, respectively. b) Western blot analysis of KARPAS-299 and MOLT-4 cell extracts was performed to measure caspase-dependent PARP cleavage (→) after treatment for 24 h with increasing concentrations of urolithin A. c) For comparison, the expression of CK2, AKT^{S129} and cleaved PARP was assessed in the nontumor cell line DAA3. Cells were exposed to 100 and 200 μM of urolithin A for 24 h.

ed with 200 μM urolithin A, healthy cells were less than 15%, and most of the cell population was distributed between late apoptosis and necrosis. By comparison, when used at lower concentrations or for shorter incubation periods, drug efficacy in these cells was lower. In leukaemia MOLT-4 cells, urolithin A activity was more dependent on drug concentration rather than on exposure time. In fact, cell survival was reduced by comparable amounts with either 100 or 200 μM urolithin A after exposure for both 24 h and 48 h, whereas differences were observed when concentrations were compared at fixed time points (50% and 10% with 100 μM and 200 μM, respectively). Additionally, whereas the cells treated with 100 μM uro-

lithin A accumulated mostly in early apoptosis (B4 quadrant in Figure 7 a), exposure to higher concentrations resulted in an increase in the cell population in late apoptosis (B2 quadrant in Figure 7 a). Consistent with these findings, exposure to urolithin A correlated with PARP cleavage in all tumor cell lines (Figure 7 b), but not in human EBV-immortalized DAA3 cells (Figure 7 c).

A comparison between nitro- and bromo-substituted urolithin A analogues (compounds **12**, **13** and **21**) was performed in order to assess the correlation between in vitro inhibitory activity and intracellular efficacy. Data reported in Figure 8 demonstrate a striking difference between compound **13** and

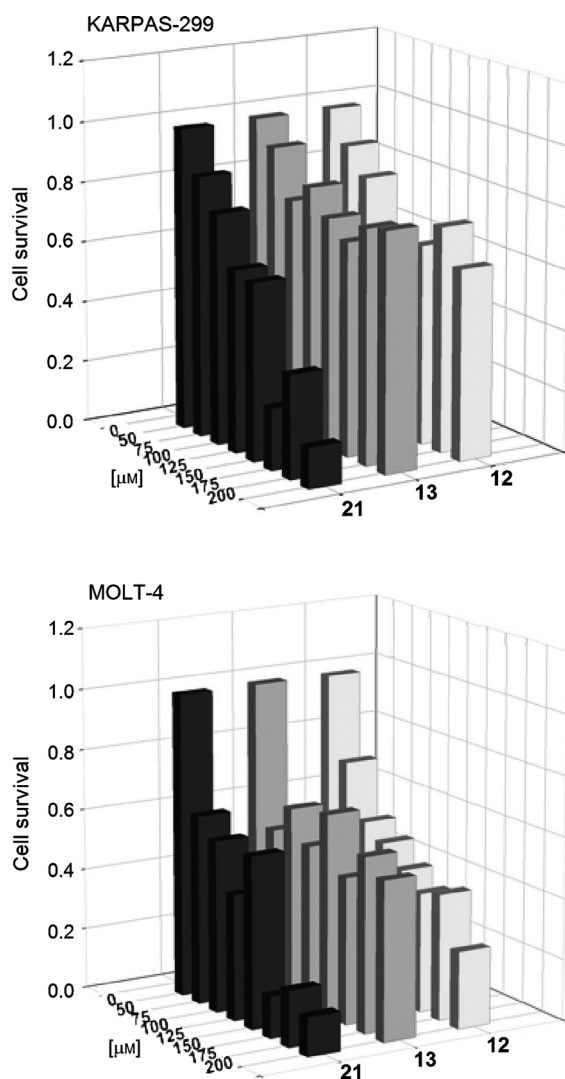


Figure 8. Cytotoxicity of urolithin A (**8**) and derivatives **12**, **13** and **21** in KARPAS-299 and MOLT-4 cells. An MTT assay was performed on cells maintained for 48 h in the presence or absence of increasing concentrations of test compound. Data represent the mean of three independent experiments performed in triplicate, using untreated samples as a control.

21, with the latter capable of reducing cell survival by up to 85% compared with untreated controls both in leukaemia (MOLT-4) and lymphoma (KARPAS-299) cell lines, while the former did not cause more than 50% growth inhibition. By comparison, the effectiveness of compound **12** was intermediate, and more cell-type dependent. MOLT-4 and KARPAS-299 were also exposed to urolithin A (**8**) and compound **21** for 48 h to assess their ability to induce apoptosis. FACS analysis gave data consistent with the results reported above, where compound **21** more strongly induced apoptosis in MOLT-4 compared to KARPAS-299 tumor cells when used at 100 μM , while urolithin A appeared to be effective at impairing cell survival in both cell lines (Table 3). In particular, when exposed to compound **21**, MOLT-4 cells underwent apoptosis in a dose-independent manner and accumulated equally in early- and late-stage apoptosis, whereas when treated with urolithin A most

Table 3. Apoptosis detection rate by annexin-V (AV) and propidium iodide (PI) staining.^[a]

Compd	Concn [μM]	AV/PI [%]			
		-/-	+/-	+/+	-/+
<i>KARPAS-299</i> ^[b]					
none	DMSO	94	3.6	1.7	0.7
8	100 ^[c]	49.4	18.4	29.6	2.7
8	200	10.1	24.4	59.5	6
21	100 ^[c]	77.5	12.3	8.6	1.6
21	200	12.8	23.5	58.2	5.5
<i>MOLT-4</i> ^[b]					
none	DMSO	91.7	7.1	1.1	0.1
8	100 ^[c]	15.6	36.9	46.8	0.74
8	200	2.4	33.0	64.5	0.06
21	100 ^[c]	18.3	45.8	35.5	0.44
21	200	12.9	49.6	37.5	0.27

[a] The association of growth inhibition with cell survival was assessed in CK2-expressing cell lines (KARPAS-299 and MOLT-4) exposed to urolithin A (**8**) or compound **21** for 48 h at the indicated concentrations (100 and 200 μM). Cell viability was measured by annexin-V (AV) and propidium iodide (PI) staining. Flow cytometry analysis was performed as described in the Experimental Section, and the proportion of healthy and dead cells was calculated. The proportion of viable (AV⁻/PI⁻), early apoptotic (AV⁺/PI⁻), late apoptotic (AV⁺/PI⁺) and necrotic cells (AV⁻/PI⁺) are reported as a percentage. [b] KARPAS-299 and MOLT-4 cells were used at a cell density of $0.5 \times 10^6 \text{ mL}^{-1}$. [c] Cells were exposed to urolithin A (**8**) or derivative **21** for 48 h at 100 μM .

of the cells accumulated in late-stage apoptosis at the higher concentration only.

Conclusions

During the last ten years, we have accumulated a lot of experience in the design and synthesis of ATP-competitive CK2 inhibitors. The recent discovery of ellagic acid as a powerful and selective inhibitor of CK2 has prompted optimization efforts to improve its activity. Here, we have shown the applicability of an X-ray structure-driven “merging approach” to discover novel CK2 inhibitors. In particular, comparing the crystallographic binding modes of both ellagic acid and DBC,^[18,19] we identified the urolithin moiety as a converging scaffold linking ellagic acid and coumarin analogues. After optimization of urolithin A, a novel potent and selective urolithin derivative was identified: 4-bromo-3,8-dihydroxy-benzo[*c*]chromen-6-one (**21**), which exhibits a K_i value of 7 nm against CK2. Although the most promising urolithin derivatives failed to exhibit potent cytotoxic effects in cell culture, these compounds could be promising in alternative therapeutic applications, where cytotoxicity is not strictly required, such as in the treatment of viral infections and inflammatory diseases like glomerulonephritis.

We are continuing the validation of our X-ray structure-driven merging approach with the aim to improve potency and selectivity of other novel protein CK2 inhibitors, hopefully with novel therapeutic applications.

Experimental Section

Chemistry

Melting points (mp) were performed on a Gallenkamp apparatus and are uncorrected. Nuclear magnetic resonance (NMR) spectra were recorded on a Bruker Avance AMX 300 spectrometer. ^1H NMR and ^{13}C NMR experiments were run using CDCl_3 , $(\text{CD}_3)_2\text{SO}$, CD_3OD or $(\text{CD}_3)_2\text{CO}$ as the solvent, and the residual solvent peak was used as an internal standard. Chemical shifts (δ) are expressed in parts per million (ppm) relative to tetramethylsilane (TMS), and spin multiplicities are indicated as: singlet (s), broad singlet (br s), doublet (d), double doublet (dd), triplet (t), and multiplet (m), and the coupling (J) values are expressed in Hertz (Hz). Analytical thin-layer chromatography (TLC) was carried out on precoated silica gel plates (Merck 60F₂₅₄), and plates were visualized under UV light at 254 nm. Column chromatography was performed using silica gel (230–400 mesh; Merck). All starting materials not described below, the solvents and the deuterated solvents were purchased from commercial sources, mainly Aldrich and Fluka. All commercially obtained reagents and solvents were used as received without additional purification, unless differently stated. Analytical HPLC was carried out on a Varian HPLC system using an HP Lichrospher C18 column (4.6 mm \times 250 mm, 100 Å) with a particle size of 5 μm . The flow rate was 1 mL min^{-1} , and the mobile phase consisted of a mixture of A = H_3PO_4 0.15% and B = MeCN; the eluate was monitored at 280 nm. Method: at time 0 min 80% A (gradient), 80 \rightarrow 10% A (20 min; linear gradient), 10% A (5 min; isocratic), and finally 10 \rightarrow 80% A (7 min; linear gradient).^[31,32] High-resolution mass spectra (HRMS) were obtained using a Mariner API-TOF instrument (PerSeptive Biosystems Inc., Framingham, USA) with electrospray ionization (ESI).

Elemental analyses of all newly synthesized CK2 inhibitors and corresponding intermediates are reported in the Supporting Information.

1,2,3,7,8-Pentahydroxy-4,9-dioxo-pyren-5,10-dione (4): A suspension of gallic acid (10 g, 0.059 mol) in H_2SO_4 96% (80 mL) and H_2O (33 mL) was cooled to -50°C and then treated with $\text{K}_2\text{S}_2\text{O}_8$ (20 g, 0.074 mol). The solution was left at 4°C overnight, after which time a precipitate had formed. The desired product was collected by filtration and recrystallized from pyridine (white solid, 2.7 g, 14%): ^1H NMR (300 MHz, $(\text{CD}_3)_2\text{SO}$): δ = 7.47 ppm (s, 1H, H6); ^{13}C NMR (300 MHz, $(\text{CD}_3)_2\text{CO}$): δ = 158.7, 158.7, 151.5, 148.9, 147.5, 146.5, 139.4, 135.2, 132.0, 123.5, 122.8, 121.4, 114.9, 108.0 ppm; HRMS: m/z $[M+H]^-$ calcd for $\text{C}_{14}\text{H}_6\text{O}_9$: 317.0142, found: 317.0031.

2,3,4,8,9,10-Hexahydroxy-dibenzo[b,d]pyran-6-one (6): A solution of KOH (22.5 g, 0.4 mol) in H_2O (30 mL) was treated with flavellagic acid (4) (3.3 g, 0.010 mol) and refluxed for 20 min. The product was extracted from the reaction mixture with Et_2O (3 \times 50 mL), and the combined organic extracts were dried with Na_2SO_4 , filtered, and concentrated in vacuo. The residue was washed with boiling water in which flavellagic acid is not soluble, and excess flavellagic acid was removed by filtration. The product was recrystallized from H_2O at RT (white solid, 2.1 g, 72%): ^1H NMR (300 MHz, $(\text{CD}_3)_2\text{SO}$): δ = 8.02 (s, 1H, H7), 7.28 ppm (s, 1H, H1); ^{13}C NMR (300 MHz, $(\text{CD}_3)_2\text{CO}$): δ = 158.7, 147.5, 146.1, 145.7, 143.6, 141.7, 135.3, 132.1, 128.4, 124.4, 115.7, 110.7, 107.8 ppm; HRMS: m/z $[M+H]^-$ calcd for $\text{C}_{13}\text{H}_8\text{O}_8$: 291.0146, found: 291.0189.

2,3,7,8-Tetramethoxy-4,9-dioxo-pyren-5,10-dione (3): A suspension of ellagic acid (1 g, 3.31 mmol) in DMF (5 mL) was cooled at 0°C and treated with NaH (0.4 g, 16.6 mmol). The suspension was stirred for 20 min at 0°C . The reaction was then treated with CH_3I

(2 mL) and stirred at 4°C for another 2 h. H_2O (50 mL) was added, and the product was extracted with CHCl_3 (3 \times 50 mL). Purification by column chromatography on silica gel (CHCl_3) and then recrystallization from toluene/ CHCl_3 (1:1) gave the desired product (white solid, 0.62 g, 52%): ^1H NMR (300 MHz, $(\text{CD}_3)_2\text{SO}$): δ = 7.56 (s, 2H, H1 and H6), 3.32 ppm (s, 12H, CH_3); ^{13}C NMR (300 MHz, $(\text{CD}_3)_2\text{CO}$): δ = 158.7, 158.7, 152.3, 152.3, 149.1, 149.1, 137.4, 137.4, 122.7, 122.7, 120.7, 120.7, 112.9, 112.9, 56.2, 56.2, 56.2, 56.2 ppm; HRMS: m/z $[M+H]^+$ calcd for $\text{C}_{18}\text{H}_{14}\text{O}_8$: 359.0761, found: 359.0660.

3,4,8,9,10-Pentahydroxy-dibenzo[b,d]pyran-6-one (5): A solution of KOH (22.5 g, 0.4 mol) in H_2O (30 mL) was treated with ellagic acid (3 g, 0.01 mol) and then refluxed for 20 min. The product was extracted from the reaction mixture with Et_2O (3 \times 50 mL), and the combined organic extracts were dried with Na_2SO_4 , filtered, and concentrated in vacuo. The residue was washed with boiling water in which ellagic acid is not soluble, and excess ellagic acid was removed by filtration. The desired product was recrystallized from H_2O at RT (white solid, 1.7 g, 62%): ^1H NMR (300 MHz, CD_3OD): δ = 8.47 (d, J = 8.9 Hz, 1H, H1), 7.41 (s, 1H, H7), 6.79 ppm (d, J = 8.9 Hz, 1H, H2); ^{13}C NMR (300 MHz, $(\text{CD}_3)_2\text{CO}$): δ = 158.9, 147.5, 146.6, 145.7, 142.2, 141.7, 139.5, 126.9, 124.5, 122.3, 115.7, 114.7, 110.7 ppm; HRMS: m/z $[M+H]^-$ calcd for $\text{C}_{13}\text{H}_8\text{O}_7$: 275.0426, found: 275.0338.

Biphenyl-2,3,4,6,2',3',4',6'-octaol (7): NaOH (35 g, 0.88 mol) was melted at 300°C and treated with ellagic acid (3 g, 0.010 mol). The reaction was stirred at the same temperature for 20 min. The mixture was cooled to RT and H_2O (140 mL) was added. The insoluble residue was removed by filtration, and the filtrate was acidified with HCl (37%) until complete precipitation of the desired product. Compound 7 was collected by filtration and dried in vacuo (white solid, 0.62 g, 22%): ^1H NMR (300 MHz, $(\text{CD}_3)_2\text{SO}$): δ = 7.56 ppm (s, 2H, H5 and H5'); ^{13}C NMR (300 MHz, $(\text{CD}_3)_2\text{CO}$): δ = 151.2 (2C), 149.0 (2C), 147.1 (2C), 129.2 (2C), 107.1 (2C), 98.0 ppm (2C); HRMS: m/z $[M+H]^-$ calcd for $\text{C}_{12}\text{H}_{10}\text{O}_8$: 281.0661, found: 281.0560.

3-Methoxy benzoic acid (23): A solution of NaOH (7.2 g, 0.18 mol) in H_2O (200 mL) was treated with 3-methoxybenzyl alcohol (5 g, 0.036 mol) and KMnO_4 (9.5 g, 0.06 mol). The mixture was heated at 100°C for 1 h (color change from green to brown due to MnO_2 formation). The warm suspension was filtered, and the filtrate was acidified with HCl (37%) until complete precipitation (pH 1). The desired product was collected by filtration and dried in an oven at 30°C (white solid, 2.7 g, 49%): ^1H NMR (300 MHz, CDCl_3): δ = 7.72 (ddd, J = 7.6, 1.5, 1.5 Hz, 1H, H6), 7.62–7.59 (m, 1H, H2), 7.39 (t, J = 8.0, 7.6 Hz, 1H, H5), 7.16–7.12 (m, 1H, H4), 3.77 ppm (s, 3H, OCH_3); ^{13}C NMR (300 MHz, $(\text{CD}_3)_2\text{CO}$): δ = 169.4, 160.6, 131.4, 129.8, 122.7, 119.6, 114.5, 56.0 ppm; HRMS: m/z $[M+H]^-$ calcd for $\text{C}_8\text{H}_8\text{O}_3$: 151.0401, found: 151.0401.

2-Bromo-5-methoxy benzoic acid (24): A solution of compound 23 (2.7 g, 0.018 mol) in AcOH (18 mL) was treated dropwise with a solution of Br_2 (2.8 g, 0.018 mol) in AcOH (9 mL). The reaction mixture was refluxed until completion (color change from orange to colorless due to consumption of bromine). Then the mixture was put into ice (5 g) until complete precipitation. The product was isolated by filtration, washed with $\text{H}_2\text{O}/\text{MeOH}$ (1:1), and dried in an oven at 30°C (white solid, 3.4 g, 82%): ^1H NMR (300 MHz, CDCl_3): δ = 7.58 (d, J = 8.8 Hz, 1H, H3), 7.50 (d, J = 3.2 Hz, 1H, H6), 6.95 (dd, J = 8.8, 3.2 Hz, 1H, H4), 3.77 ppm (s, 3H, OCH_3); ^{13}C NMR (300 MHz, $(\text{CD}_3)_2\text{CO}$): δ = 169.4, 159.7, 133.0, 132.6, 121.8, 116.7, 115.1, 56.0 ppm; HRMS: m/z $[M+H]^-$ calcd for $\text{C}_8\text{H}_7\text{BrO}_3$: 230.9486, found: 230.9440.

3-Hydroxy-8-methoxy-dibenzo[*b,d*]pyran-6-one (9)^[33] A solution of **24** (3.4 g, 0.015 mol), resorcinol (3.2 g, 0.029 mol) and NaOH (1.2 g, 0.029 mol) in water (15 mL) was refluxed for 20 min. Then a 5% aqueous solution of CuSO₄ (6.2 mL) was added to the mixture, and the reaction was heated at reflux for an additional 1 h. Completion of the reaction was determined by TLC (CHCl₃/MeOH, 9:1). The suspension obtained was filtered, and the solid residue was dried to give **9** (white solid, 1.8 g, 51%): ¹H NMR (300 MHz, (CD₃)₂SO): δ = 10.21 (s, 1H, OH), 8.21 (d, *J* = 8.9 Hz, 1H, H10), 8.09 (d, *J* = 8.4 Hz, 1H, H1), 7.60 (d, *J* = 2.7 Hz, 1H, H7), 7.49 (dd, *J* = 8.9, 2.7 Hz, 1H, H9), 6.83 (dd, *J* = 8.4, 2.4 Hz, 1H, H2), 6.75 (d, *J* = 2.4 Hz, 1H, H4), 3.89 ppm (s, 3H, OCH₃); ¹³C NMR (300 MHz, (CD₃)₂SO): δ = 160.4, 158.8, 158.4, 151.1, 128.4, 124.1, 123.9, 123.5, 119.9, 113.0, 110.7, 109.4, 102.7, 55.5 ppm; HRMS: *m/z* [*M*+H]⁻ calcd for C₁₄H₁₀O₄: 241.0506, found: 241.0488.

3,8-Dihydroxy-dibenzo[*b,d*]pyran-6-one (8): A suspension of **9** (1.8 g, 7.4 mmol) in an azeotropic mixture of HBr (40 mL) and AcOH (80 mL) was refluxed for 11 h. Completion of the reaction was determined by TLC (CHCl₃/MeOH, 9:1). The mixture was put into the ice (5 g) until complete precipitation of the desired product, which was then isolated by filtration and dried (white solid, 1.25 g, 74%): ¹H NMR (300 MHz, (CD₃)₂SO): δ = 8.11 (d, *J* = 8.8 Hz, 1H, H10), 8.02 (d, *J* = 8.7 Hz, 1H, H1), 7.51 (d, *J* = 2.6 Hz, 1H, H7), 7.32 (dd, *J* = 8.8, 2.6 Hz, 1H, H9), 6.81 (dd, *J* = 8.7, 2.4 Hz, 1H, H2), 6.72 ppm (d, *J* = 2.4 Hz, 1H, H4); ¹³C NMR (300 MHz, (CD₃)₂SO): δ = 160.5, 158.5, 156.9, 150.8, 126.8, 124.1, 123.9, 123.2, 120.1, 113.4, 112.5, 109.7, 102.3 ppm; HRMS: *m/z* [*M*+H]⁻ calcd for C₁₃H₈O₄: 227.0350, found: 227.0334.

3,8-Dimethoxy-dibenzo[*b,d*]pyran-6-one (10): K₂CO₃ (31 g, 0.225 mol) and dimethylsulfate (26.5 g, 0.21 mol) were added to a solution of **10** (0.5 g, 2.1 mmol) in acetone (300 mL). The reaction mixture was refluxed for 40 min. Completion of the reaction was determined by TLC (CHCl₃/MeOH, 9:1). The solid salts were removed by filtration, and the filtrate was concentrated in vacuo. The solid residue was solubilized in EtOAc (30 mL) and washed with water (3 × 50 mL). The organic phase was separated, dried (Na₂SO₄), filtered and concentrated in vacuo (white solid, 0.102 g, 19%): ¹H NMR (300 MHz, CDCl₃): δ = 7.90 (d, *J* = 8.9 Hz, 1H), 7.84 (d, *J* = 8.7 Hz, 1H), 7.74 (d, *J* = 2.8 Hz, 1H), 7.35 (dd, *J* = 8.9, 2.8 Hz, 1H), 6.88 (dd, *J* = 8.7, 2.6 Hz, 1H), 6.84 (d, *J* = 2.6 Hz, 1H), 3.95 (s, 3H), 3.87 ppm (s, 3H); ¹³C NMR (300 MHz, CDCl₃): δ = 161.6, 160.7, 159.2, 151.7, 128.6, 124.5, 123.1, 122.8, 121.0, 112.4, 111.3, 111.0, 101.9, 55.7, 55.7 ppm; HRMS: *m/z* [*M*+H]⁺ calcd for C₁₅H₁₂O₄: 257.0808, found: 257.0790

3,8-Dihydroxy-2,4,7,9-tetranitro-6H-dibenzo[*b,d*]pyran-6-one (19): A solution of **11** (0.5 g, 2.2 mmol) in AcOH (25 mL) was treated with HNO₃ (65%, 0.83 g, 13.2 mmol) and heated at 50 °C for 4 h. Completion of the reaction was determined by TLC (EtOAc/*n*-hexane/MeOH, 7:2:1). Then the solvent was evaporated in vacuo, and the residue was crystallized from AcOH (yellow solid, 0.2 g, 22%): ¹H NMR (300 MHz, (CD₃)₂CO): δ = 9.51 (s, 1H, H10), 9.49 ppm (s, 1H, H1); ¹³C NMR (300 MHz, (CD₃)₂CO): δ = 154.9, 149.7, 149.0, 147.7, 142.6, 134.4, 126.8, 125.7, 124.5, 123.5, 122.4, 119.0, 112.0 ppm; HRMS: *m/z* [*M*+H]⁻ calcd for C₁₃H₄N₄O₁₂: 407.0107, found: 407.0173.

3-Hydroxy-8-methoxy-2-nitro-6H-dibenzo[*b,d*]pyran-6-one (15) and 3-hydroxy-8-methoxy-2,4-dinitro-6H-dibenzo[*b,d*]pyran-6-one (16): A solution of **10** (0.5 g, 2.1 mmol) in AcOH (12 mL) was treated with HNO₃ 65% (0.27 g, 4.3 mmol) and heated at 50 °C for 4 h. Completion of the reaction was determined by TLC (CHCl₃/MeOH, 9:1). The suspension obtained was filtered, and the solid

residue was dried to give a mixture of **15** and **16**. The two products were separated by column chromatography on silica gel (CHCl₃/MeOH, 9:1).

Compound **15** (yellow solid, 0.078 g, 13%): ¹H NMR (300 MHz, (CD₃)₂CO): δ = 8.81 (s, 1H, H1), 8.37 (d, *J* = 8.9 Hz, 1H, H10), 7.62 (d, *J* = 2.8 Hz, 1H, H7), 7.53 (dd, *J* = 8.9, 2.8 Hz, 1H, H9), 7.03 (s, 1H, H4), 4.01 ppm (s, 3H, OCH₃); ¹³C NMR (300 MHz, (CD₃)₂SO): δ = 161.7, 161.6, 155.7, 155.0, 137.3, 128.9, 128.7, 126.0, 123.0, 122.8, 113.5, 112.5, 108.0, 57.9 ppm; HRMS: *m/z* [*M*+H]⁻ calcd for C₁₄H₉NO₆: 286.0357, found: 286.0383.

Compound **16** (yellow solid, 0.41 g, 59%): ¹H NMR (300 MHz, (CD₃)₂CO): δ = 9.05 (s, 1H, H1), 8.45 (d, *J* = 8.9 Hz, 1H, H10), 7.72 (d, *J* = 2.8 Hz, 1H, H7), 7.59 (dd, *J* = 8.9, 2.8 Hz, 1H, H9), 4.01 ppm (s, 3H, OCH₃); ¹³C NMR (300 MHz, (CD₃)₂SO): δ = 171.9, 159.2, 158.2, 151.6, 145.4, 135.8, 126.6, 124.5, 124.1, 121.3, 119.9, 111.3, 106.4, 55.6 ppm; HRMS: *m/z* [*M*+H]⁻ calcd for C₁₄H₈N₂O₈: 331.0208, found: 331.0195.

3,8-Dihydroxy-2,4-dinitro-6H-dibenzo[*b,d*]pyran-6-one (14): A 50 mL flask was charged with excess pyridine chlorohydrate (0.7 g, 6 mmol) and **16** (0.2 g, 0.6 mmol), and the mixture was heated to 210 °C to achieve complete solubilization of pyridine chlorohydrate and then stirred at this temperature for 4 h. The reaction mixture was cooled during which pyridine chlorohydrate resolidified. EtOAc (20 mL) was added to the suspension, and the organic solution was washed with water (5 × 20 mL) to removed excess pyridine chlorohydrate. The organic phase was separated, dried (Na₂SO₄), filtered and concentrated in vacuo. The crude was purified by column chromatography on silica gel (CHCl₃/MeOH, 9:1) to give **14** (yellow solid, 60 mg, 31%): ¹H NMR (300 MHz, (CD₃)₂CO): δ = 8.96 (s, 1H, H1), 8.56 (d, *J* = 8.9 Hz, 1H, H10), 7.69 (d, *J* = 2.8 Hz, 1H, H7), 7.43 ppm (dd, *J* = 8.9, 2.8 Hz, 1H, H9); ¹³C NMR (300 MHz, (CD₃)₂SO): δ = 158.7, 157.4, 154.7, 149.4, 135.2, 131.1, 130.5, 130.0, 129.3, 127.6, 127.4, 121.7, 116.6 ppm; HRMS: *m/z* [*M*+H]⁻ calcd for C₁₃H₆N₂O₈: 317.2294, found: 317.2369.

2-Nitro-resorcinol (25): Resorcinol (5 g, 0.05 mol) was dissolved in hot H₂SO₄ (96%, 36 mL, 33.84 g, 0.35 mol). After 5 min, resorcinol-H₂SO₄ began to precipitate out of solution. The suspension was cooled to RT with formation of a white precipitate. The suspension was treated with HNO₃ (65%, 2.84 g, 0.05 mol) and H₂SO₄ (9.05 g, 0.09 mol) under strong stirring until complete solubilization was observed. Stirring was then suspended and ice (60 g per 100 g of solution) was added slowly. The reaction mixture was refluxed, and the product was obtained by distillation. The product was further purified by crystallization from abs EtOH to give **25** as red needles (3.8 g, 60%): ¹H NMR (300 MHz, (CD₃)₂CO): δ = 7.40 (t, *J* = 8.4 Hz, 1H, H5), 6.61 ppm (d, *J* = 8.4 Hz, 2H, H4 and H6); ¹³C NMR (300 MHz, (CD₃)₂SO): δ = 154.6, 154.6, 137.8, 122.9, 109.5, 109.5 ppm; HRMS: *m/z* [*M*+H]⁻ calcd for C₆H₅NO₄: 154.0146, found: 154.0157.

3-Hydroxy-4-nitro-dibenzo[*b,d*]pyran-6-one (17): A solution of 2-bromo-benzoic acid (1 g, 0.005 mol), 2-nitro-resorcinol (1 g, 0.006 mol) and NaOH (0.4 g, 0.010 mol) in water (20 mL) was refluxed for 30 min. Then a 10% aqueous solution of CuSO₄ (0.5 mL) was added to the mixture, and the reaction was refluxed for an addition 1 h. Completion of the reaction was determined by TLC (CHCl₃/acetone, 1:1). The suspension was filtered, and the solid residue was dried in an oven at 30 °C. Purification by column chromatography on silica gel (CHCl₃/MeOH, 9:1) gave the title compound (white solid, 0.2 g, 16%): ¹H NMR (300 MHz, (CD₃)₂CO): δ = 8.16 (dd, *J* = 8.9, 2.7 Hz, 1H, H7), 7.82 (d, *J* = 9.0 Hz, 1H, H1), 7.53–7.50 (m, 2H, H9, H10), 7.37–7.32 (m, 1H, H8), 6.96 ppm (d, *J* = 9.0 Hz, 1H,

H2); ^{13}C NMR (300 MHz, $(\text{CD}_3)_2\text{CO}$): δ = 160.7, 154.2, 145.7, 137.3, 136.3, 132.0, 130.9, 130.3, 127.4, 123.7, 121.2, 115.7, 111.7 ppm; HRMS: m/z $[M+H]^-$ calcd for $\text{C}_{13}\text{H}_7\text{NO}_5$: 256.0251, found: 256.0130.

3-Hydroxy-dibenzo[*b,d*]pyran-6-one (11): A solution of 2-bromo-benzoic acid (2 g, 0.010 mol), resorcinol (2 g, 0.018 mol) and NaOH (0.4 g, 0.010 mol) in water (20 mL) was refluxed for 30 min. Then a 10% aqueous solution of CuSO_4 (0.5 mL) was added to the mixture, and the reaction was refluxed for an additional 1 h. Completion of the reaction was determined by TLC ($\text{CHCl}_3/\text{acetone}$, 1:1). The suspension was filtered, and the solid was dried in an oven at 30 °C. Purification by column chromatography on silica gel ($\text{CHCl}_3/\text{MeOH}$, 9:1) gave the title compound (white solid, 740 mg, 35%): ^1H NMR (300 MHz, $(\text{CD}_3)_2\text{CO}$): δ = 8.20 (dd, J = 8.9, 2.7 Hz, 1H, H7), 7.63–7.57 (m, 2H, H10, H9), 7.47–7.42 (m, 2H, H1, H8), 6.69 (dd, J = 9.0, 2.1 Hz, 1H, H2), 6.67 ppm (d, J = 2.1 Hz, 1H, H4) ^{13}C NMR (300 MHz, $(\text{CD}_3)_2\text{CO}$): δ = 160.7, 157.9, 153.0, 135.6, 134.6, 130.8, 129.8, 129.0, 127.9, 127.7, 125.0, 113.2, 109.8 ppm; HRMS: m/z $[M+H]^-$ calcd for $\text{C}_{13}\text{H}_8\text{O}_3$: 211.4534, found: 211.4237.

3-Hydroxy-4-nitro-8-methoxy-dibenzo[*b,d*]pyran-6-one (12): A solution of 2-bromo-5-methoxy-benzoic acid (1 g, 0.004 mol), 2-nitro-resorcinol (0.8 g, 0.005 mol) and NaOH (0.4 g, 0.010 mol) in water (20 mL) was refluxed for 30 min. Then a 10% aqueous solution of CuSO_4 (0.5 mL) was added to the mixture, and the reaction was refluxed for an additional 1 h. Completion of the reaction was determined by TLC ($\text{CHCl}_3/\text{acetone}$, 1:1). The suspension obtained was filtered, and the solid residue was dried in an oven at 30 °C. Purification by column chromatography on silica gel ($\text{CHCl}_3/\text{MeOH}$, 8:2) gave the title compound (white solid, 600 mg, 52%): ^1H NMR (300 MHz, $(\text{CD}_3)_2\text{SO}$): δ = 8.29 (d, J = 8.8 Hz, 1H, H1), 8.26 (d, J = 8.8 Hz, 1H, H10), 7.62 (d, J = 2.9 Hz, 1H, H7), 7.55 (dd, J = 8.8, 2.9 Hz, 1H, H9), 7.06 (d, J = 8.8 Hz, 1H, H2), 3.91 ppm (s, 3H, OCH_3); ^{13}C NMR (300 MHz, $(\text{CD}_3)_2\text{SO}$): δ = 159.2, 158.7, 150.3, 148.5, 142.0, 127.1, 125.4, 124.2, 124.1, 120.0, 113.4, 111.1, 109.8, 55.65 ppm; HRMS: m/z $[M+H]^-$ calcd for $\text{C}_{14}\text{H}_9\text{NO}_6$: 286.0984, found: 286.0367.

2,4-Dibromo-3-hydroxy-8-methoxy-6H-dibenzo[*b,d*]pyran-6-one (18): A solution of **9** (1 g, 4.1 mmol) in CCl_4 (40 mL) was treated with NBS (0.73 g, 4.1 mmol) and benzoyl peroxide (radical initiator) (10 mg, 0.041 mmol), and the reaction was refluxed for 2 h. Completion of the reaction was determined by TLC (*n*-hexane/EtOAc, 8:2). The suspension obtained was filtered, and the solid residue was dried in an oven at 30 °C. Purification by column chromatography on silica gel ($\text{CHCl}_3/\text{EtOAc}$, 9:1) gave the desired product **18** (white solid, 0.078 g, 30%): ^1H NMR (300 MHz, $(\text{CD}_3)_2\text{CO}$): δ = 8.11 (s, 1H, H1), 7.90 (d, J = 8.9 Hz, 1H, H10), 7.70 (d, J = 2.8 Hz, 1H, H7), 7.42 (dd, J = 8.9, 2.8 Hz, 1H, H9), 3.95 ppm (s, 3H, OCH_3); ^{13}C NMR (300 MHz, $(\text{CD}_3)_2\text{SO}$): δ = 159.5, 158.8, 155.7, 151.8, 134.4, 130.1, 130.0, 128.8, 127.4, 120.0, 115.0, 114.6, 113.4, 56.0 ppm; HRMS: m/z $[M+H]^-$ calcd for $\text{C}_{14}\text{H}_8\text{Br}_2\text{O}_4$: 399.0453, found: 399.0857.

2,4,6-Tribromo-resorcinol (26): Br_2 (4.5 mL, 14 g, 0.087 mol) was added dropwise to a suspension of resorcinol (3 g, 0.027 mol) in CHCl_3 (45 mL). The reaction mixture was refluxed for 2 h. Completion of the reaction was determined by TLC ($\text{CHCl}_3/\text{MeOH}$, 9:1). The solvent was partially evaporated in vacuo (50%), and the mixture was left at 4 °C to crystallize overnight until complete crystallization. The crystalline product was isolated by filtration and dried to give **26** (white solid, 5.4 g, 58%): ^1H NMR (300 MHz, CDCl_3): δ = 7.60 (s, 1H, H5), 5.92 ppm (s, 2H, OH); ^{13}C NMR (300 MHz, $(\text{CD}_3)_2\text{SO}$): δ = 153.0 (2C), 136.6, 110.8 (2C), 110.7 ppm; HRMS: m/z $[M+H]^-$ calcd for $\text{C}_6\text{H}_3\text{Br}_3\text{O}_2$: 345.4014, found: 345.4057.

2-Bromo-resorcinol (27): A suspension of 2,4,6-tribromo-resorcinol (2 g, 0.0058 mol) in H_2O (40 mL) was treated with Na_2SO_3 (21.8 g,

0.173 mol) in H_2O (60 mL). The reaction mixture was acidified to pH 2 by dropwise addition of H_2SO_4 and then refluxed for 12 h. Completion of the reaction was determined by TLC ($\text{CHCl}_3/\text{MeOH}$, 9:1). The reaction mixture was cooled to RT and neutralized by dropwise addition of aqueous NaHCO_3 (1 M). The aqueous reaction mixture was extracted with toluene (3 × 60 mL), and the organic phase was separated, dried (Na_2SO_4), filtered and concentrated in vacuo to give **27** (white solid, 0.702 g, 64%): ^1H NMR (300 MHz, CDCl_3): δ = 6.94 (t, J = 8.1 Hz, 1H, H5), 6.39 ppm (d, J = 8.1 Hz, 2H, H4, H6); ^{13}C NMR (300 MHz, $(\text{CD}_3)_2\text{SO}$): δ = 158.1 (2C), 130.6, 110.7 (2C), 106.3 ppm; HRMS: m/z $[M+H]^-$ calcd for $\text{C}_6\text{H}_5\text{BrO}_2$: 188.0014, found: 188.0072.

4-Bromo-3-hydroxy-8-methoxy-dibenzo[*b,d*]pyran-6-one (13): A solution of 2-bromo-5-methoxy-benzoic acid (200 mg, 0.866 mmol), 2-nitro-resorcinol (327 mg, 1.732 mmol) and NaOH (69 mg, 1.732 mmol) in water (10 mL) was refluxed for 30 min. Then a 10% aqueous solution of CuSO_4 (0.5 mL) was added to the mixture, and the reaction was refluxed for an additional 1 h. Completion of the reaction was determined by TLC ($\text{CHCl}_3/\text{MeOH}$, 9:1). The reaction mixture was cooled to RT, and the precipitate was collected by filtration and dried in vacuo. Purification by column chromatography on silica gel ($\text{CHCl}_3/\text{MeOH}$, 95:5) gave **13** (white solid, 81 mg, 29%): ^1H NMR (300 MHz, CDCl_3): δ = 7.93 (d, J = 8.9 Hz, 1H, H1), 7.84 (d, J = 8.8 Hz, 1H, H10), 7.79 (d, J = 2.8 Hz, 1H, H7), 7.40 (dd, J = 8.8, 2.8 Hz, 1H, H9), 7.05 (d, J = 8.8 Hz, 1H, H2), 5.89 (br s, 1H, OH), 3.94 ppm (s, 3H, OCH_3); ^{13}C NMR (300 MHz, $(\text{CD}_3)_2\text{SO}$): δ = 159.5, 158.7, 156.7, 156.0, 130.1, 128.8, 128.8, 127.8, 127.4, 120.0, 115.4, 115.1, 112.4, 56.0 ppm; HRMS: m/z $[M+H]^-$ calcd for $\text{C}_{14}\text{H}_9\text{BrO}_4$: 320.1454, found: 320.1398.

3-Hydroxy-8-methoxy-4-methyl-dibenzo[*b,d*]pyran-6-one (20): A solution of 2-bromo-5-methoxy-benzoic acid (280 mg, 1.206 mmol), 2-methyl-resorcinol (300 mg, 2.416 mmol) and NaOH (96 g, 2.4 mmol) in water (10 mL) was refluxed for 30 min. Then a 10% aqueous solution of CuSO_4 (0.5 mL) was added to the mixture, and the reaction was refluxed for an additional 1 h. Completion of the reaction was determined by TLC ($\text{CHCl}_3/\text{MeOH}$, 9:1). The reaction mixture was cooled to RT, and the precipitate was isolated by filtration and dried in vacuo. Purification by column chromatography on silica gel ($\text{CHCl}_3/\text{MeOH}$, 9:1) gave **20** (white solid, 100 mg, 32%): ^1H NMR (300 MHz, $(\text{CD}_3)_2\text{CO}$): δ = 8.16 (d, J = 8.9 Hz, 1H, H10), 7.89 (d, J = 8.7 Hz, 1H, H1), 7.70 (d, J = 2.8 Hz, 1H, H7), 7.45 (dd, J = 8.9, 2.8 Hz, 1H, H9), 6.94 (d, J = 8.7 Hz, 1H, H2), 3.85 (s, 3H, OCH_3), 2.31 ppm (s, 3H, CH_3); ^{13}C NMR (300 MHz, $(\text{CD}_3)_2\text{CO}$): δ = 159.5, 158.7, 155.5, 154.1, 130.1, 128.8, 127.3, 126.7, 125.5, 121.2, 120.1, 115.0, 113.1, 56.0, 4.4 ppm; HRMS: m/z $[M+H]^-$ calcd for $\text{C}_{15}\text{H}_{12}\text{O}_4$: 255.0663, found: 255.0581.

3,8-Dihydroxy-4-methyl-6H-dibenzo[*b,d*]pyran-6-one (22): A suspension of **20** (0.1 g, 0.39 mmol) in an azeotropic mixture of HBr (4 mL) and AcOH (8 mL) was refluxed for 11 h. Completion of the reaction was determined by TLC ($\text{CHCl}_3/\text{EtOAc}$, 7:3). The mixture was put into the ice (2 g) until complete precipitation. The solid was isolated by filtration and further purified by column chromatography on silica gel ($\text{CHCl}_3/\text{EtOAc}$, 7:3) to give the title compound (white solid, 53 g, 56%): ^1H NMR (300 MHz, $(\text{CD}_3)_2\text{CO}$): δ = 8.96 (s, 1H, H1), 8.56 (d, J = 8.9 Hz, 1H, H10), 7.69 (d, J = 2.8 Hz, 1H, H7), 7.43 ppm (dd, J = 8.9, 2.8 Hz, 1H, H9); ^{13}C NMR (300 MHz, $(\text{CD}_3)_2\text{CO}$): δ = 158.7, 157.3, 155.6, 154.3, 132.4, 129.3, 127.6, 126.7, 125.5, 121.7, 121.3, 116.6, 113.2, 4.5 ppm; HRMS: m/z $[M+H]^+$ calcd for $\text{C}_{14}\text{H}_{10}\text{O}_4$: 243.0663, found: 243.0629.

Biology

Source and purification of protein kinases: Native CK1 and CK2 were purified from rat liver.^[34] Recombinant human CK2 subunit α was expressed in *Escherichia coli* and purified as described previously.^[35] Protein kinase A (PKA) was purchased from Sigma–Aldrich, and recombinant human GSK3 β was purchased from Upstate Biotechnology Inc. Recombinant human DYRK1a was kindly provided by Prof. Dr. Walter Becker (Institut für Pharmakologie und Toxikologie, Universitätsklinikum Aachen, Germany). The source of all of the other protein kinases used for specificity assays is as described previously.^[36]

Phosphorylation assay: CK2 and CK1 phosphorylation assays were carried out at 37 °C in the presence of increasing amounts of test compound in a final volume of 25 μ L containing 50 mM Tris-HCl (pH 7.5), 100 mM NaCl, 12 mM MgCl₂, 0.02 mM [³²P]ATP (500–1000 cpm pmol⁻¹), unless otherwise indicated. The phosphorylatable substrates were the synthetic peptide substrate RRRADSDDDDD (100 μ M) and RRKHAAGDDDDAYSITA (200 μ M) for CK2 and all CK1, respectively. Reaction started with the addition of kinase and was stopped after 10 min by addition of orthophosphoric acid (0.5 M, 5 μ L) before spotting aliquots onto phosphocellulose filters. The filters were then washed with H₃PO₄ (75 mM, 4 \times 5–10 mL) and MeOH, and then dried before counting.^[35] Each determination was repeated in three independent experiments and the mean of the data were calculated. PKA was assayed in the presence of 1 μ M cAMP under identical conditions by omitting NaCl and using the synthetic peptide substrate ALRRASLGAA. GSK3 β inhibition was determined using protein phosphatase inhibitor-2 (I-2) as a phosphoacceptor substrate following sodium dodecyl sulfate (SDS)-polyacrylamide gel electrophoresis (PAGE) of the radiolabeled samples. DYRK1A was assayed using the peptide RRRFRPASPLRGPPK. PIM1 activity was determined by following the same procedure, incubating the kinase in the presence of 50 mM Tris-HCl (pH 7.5), 0.1% (v/v) 2-mercaptoethanol, 0.1 mM ethylene glycol tetraacetic acid (EGTA), 30 μ M synthetic peptide substrate RRRRQTSMTD and 100 μ M [³²P]ATP. HIPK2 activity was determined under the same conditions used for PIM1 assays, using 20 μ M ATP and 10 μ g myelin basic protein (MBP) as the phosphorylatable substrate. PKA was assayed in the presence of 1 μ M cAMP under identical conditions, omitting NaCl and using synthetic peptide substrate ALRRASLGAA. Aurora-A was assayed under the same condition used for PKA without cAMP.

Kinetic determination: Initial velocities were determined at each of the substrate concentration tested. K_M values were calculated in the absence or presence of increasing inhibitor concentrations from Lineweaver–Burk double-reciprocal plots of the data. Inhibition constants (K_i) were calculated by linear regression analysis of K_M/V_{max} versus inhibitor concentration plots. K_i values were also calculated using the Cheng–Prusoff equation^[37] by determining the IC₅₀ value for each compound at 1 μ M ATP, assuming a competitive mechanism of inhibition.

Cell viability assay: Human anaplastic large-cell lymphoma (ALCL) cell lines KARPAS-299 and MAC-2A were maintained in RPMI-1640 containing 15% heat-inactivated fetal calf serum (FCS), 2 mmol L⁻¹ glutamine, 100 U mL⁻¹ penicillin, and 100 μ g mL⁻¹ streptomycin under standard tissue culture conditions. Acute lymphoblastic leukemia (ALL) cell lines MOLT-4 and HL-60 were maintained in RPMI-1640 containing 10% heat-inactivated FCS.

Cell viability was measured using an MTT assay. Briefly, 0.1 \times 10⁵ cells were seeded into 96-well microculture plates 12 h before addition of the test compound. Cells were cultured under standard

conditions in 200 μ L of complete RPMI-1640 medium for 48 h in the presence or absence of test compound. 3-(4,5-Dimethylthiazol-2-yl)-2,5-diphenyltetrazolium bromide (MTT) solution (20 μ L, 5 mg mL⁻¹) was added to the cell suspension and left for 4 h. The intracellular formazan crystals were dissolved with DMSO (150 μ L), and the optical density was measured using a Victor3 multilabel counter spectrophotometer at 540 nm. Values represent the mean (\pm SD) of triplicate cultures of three independent experiments.

Immunoblotting: Exponentially growing ALCL and ALL cells were treated with test compound as described above. At the end of treatment, the cells were washed twice with ice-cold 1x phosphate buffered saline (PBS), resuspended in RIPA buffer (50 mM Tris-HCl (pH 7.5), 150 mM NaCl, 1 mM EDTA, 0.1% SDS, 0.5% deoxycholic acid, 1% Triton-X100) and kept on ice for 20 min. Cells were then clarified by high-speed centrifugation (14,000 g for 30 min at 4 °C). After centrifugation, supernatants were recovered and 60 μ g of lysates were loaded onto 12% SDS-PAGE, electrotransferred to polyvinylidene fluoride (PVDF) membranes, and probed for CK2 (Sigma), phosphorylated AKT (AKT^{S129}, Cell Signaling Technology, Inc.) or full-length and cleaved PARP (Cell Signaling Technology, Inc.) as indicated. Proteins were visualized by chemiluminescence using a commercial kit (Chemicon) and Amersham Hyperfilms (GE Healthcare), and when indicated, protein bands were quantified using ImageJ 1.42q software (US National Institutes of Health).

Assessment of apoptosis: To measure drug-induced apoptosis, ALCL and ALL cells were treated with test compounds and stained with annexin-V-FITC/propidium iodide prior to flow cytometry analysis. Briefly, cells were harvested, washed with PBS, and stained (0.5 \times 10⁶) with annexin-V (5 μ L) and propidium iodide (5 μ g mL⁻¹, 5 μ L) in 1 mL of 1x annexin binding buffer (10 mM HEPES (pH 7.4), 140 mM NaOH, 2.5 mM CaCl₂) (Immunostep Research, Spain). Cells were left at RT in the dark for 15 min, and apoptosis was measured using a FACSCalibur flow cytometer (BD Biosciences, USA). Early apoptotic (AV⁺/PI⁻) and late apoptotic cells (AV⁺/PI⁺) were included in the analysis.

Molecular modeling

The crystal structure of human CK2 subunit α was retrieved from the Protein Data Bank (PDB: 2ZJW^[18]) and processed in order to remove the ligand (ellagic acid) and water molecules. Hydrogen atoms were added using standard geometries to the protein structure with the MOE program.^[38] To minimize contacts between hydrogen atoms, the structures were subjected to Amber94 force-field minimization until the root mean square (rms) of the conjugate gradient was < 0.1 kcal mol⁻¹ Å⁻¹, keeping heavy atoms fixed in their crystallographic positions.^[38]

Ligand structures were built using the MOE builder tool, part of the MOE suite,^[38] and were subjected to MMFF94x energy minimization until the rms of the conjugate gradient was 0.05 kcal mol⁻¹ Å⁻¹. Charges were calculated using ESP methodology.

Three different programs were used to calibrate our docking protocols: MOE-Dock,^[38] GOLD^[39] and Glide.^[40] To select the best performing docking protocol, ellagic acid was re-docked to the crystal structure of human CK2 subunit α (PDB: 2ZJW) with several combinations of docking algorithms and scoring functions (see Tables S2 and S3 in the Supporting Information).

Abbreviations

Casein kinase 2 (CK2); 3,8-dibromo-7-hydroxy-4-methylchromen-2-one (DBC); 1,8-dihydroxy-4-nitroxanthene-9-one (MNX); 8-hydroxy-4-methyl-9-nitrobenzo[g]chromen-2-one (NBC); tetrabromocinnamic acid (TBCA); root mean square deviation (RMSD); standard error of the mean (SEM); water (W).

Acknowledgements

The molecular modeling work coordinated by S.M. was made possible by financial support from the University of Padova (Italy) and the Italian Ministry for University and Research (MIUR) (PRIN2008; protocol: 200834TC4L_002). S.M. is very grateful for the scientific and technical partnership with Chemical Computing Group (Montreal, Canada). The authors also thank Dr. Stefania Sarno (Department of Biological Chemistry, University of Padova, Italy) for the kind donation of DIRK1a and CK2 α kinase.

Keywords: cancer · drug design · kinase inhibitors · protein kinase CK2 · urolithin A

- [1] G. Cozza, A. Bortolato, S. Moro, *Med. Res. Rev.* **2010**, *30*, 419–462.
- [2] G. Cozza, F. Meggio, S. Moro, *Curr. Med. Chem.* **2011**, *18*, 2867–2884.
- [3] D. W. Litchfield, *Biochem. J.* **2003**, *369*, 1–15.
- [4] D. C. Seldin, P. Leder, *Science* **1995**, *267*, 894–897.
- [5] M. A. Kelliher, D. C. Seldin, P. Leder, *EMBO J.* **1996**, *15*, 5160–5166.
- [6] E. Landesman-Bollag, P. L. Channavajhala, R. D. Cardiff, D. C. Seldin, *Oncogene* **1998**, *16*, 2965–2974.
- [7] M. Orlandini, F. Semplici, R. Ferruzzi, F. Meggio, L. A. Pinna, S. Oliviero, *J. Biol. Chem.* **1998**, *273*, 21291–21297.
- [8] C. Guo, S. Yu, A. T. Davis, H. Wang, J. E. Green, K. Ahmed, *J. Biol. Chem.* **2001**, *276*, 5992–5999.
- [9] S. Tawfic, S. Yu, H. Wang, R. Faust, A. Davis, K. Ahmed, *Histol. Histopathol.* **2001**, *16*, 573–582.
- [10] G. M. Unger, A. T. Davis, J. W. Slaton, K. Ahmed, *Curr. Cancer Drug Targets* **2004**, *4*, 77–84.
- [11] M. Yamada, S. Katsuma, T. Adachi, A. Hirasawa, S. Shiojima, T. Kadowaki, Y. Okuno, T. A. Koshimizu, S. Fujii, Y. Sekiya, Y. Miyamoto, M. Tamura, W. Yumura, H. Nihei, M. Kobayashi, G. Tsujimoto, *Proc. Natl. Acad. Sci. USA* **2005**, *102*, 7736–7741.
- [12] E. De Moliner, S. Moro, S. Sarno, G. Zagotto, G. Zanotti, L. A. Pinna, R. Battistutta, *J. Biol. Chem.* **2003**, *278*, 1831–1836.
- [13] F. Meggio, M. A. Pagano, S. Moro, G. Zagotto, M. Ruzzene, S. Sarno, G. Cozza, J. Bain, M. Elliott, A. D. Deana, A. M. Brunati, L. A. Pinna, *Biochemistry* **2004**, *43*, 12931–12936.
- [14] G. Cozza, P. Bonvini, E. Zorzi, G. Poletto, M. A. Pagano, S. Sarno, A. Donella-Deana, G. Zagotto, A. Rosolen, L. A. Pinna, F. Meggio, S. Moro, *J. Med. Chem.* **2006**, *49*, 2363–2366.
- [15] S. Sarno, S. Moro, F. Meggio, G. Zagotto, D. Dal Ben, P. Ghisellini, R. Battistutta, G. Zanotti, L. A. Pinna, *Pharmacol. Ther.* **2002**, *93*, 159–168.
- [16] M. A. Pagano, G. Poletto, G. Di Maira, G. Cozza, M. Ruzzene, S. Sarno, J. Bain, M. Elliott, S. Moro, G. Zagotto, F. Meggio, L. A. Pinna, *ChemBioChem* **2007**, *8*, 129–139.
- [17] G. Cozza, M. Mazzorana, E. Papinutto, J. Bain, M. Elliott, G. di Maira, A. Gianoncelli, M. A. Pagano, S. Sarno, M. Ruzzene, R. Battistutta, F. Meggio, S. Moro, G. Zagotto, L. A. Pinna, *Biochem. J.* **2009**, *421*, 387–395.
- [18] Y. Sekiguchi, T. Nakaniwa, T. Kinoshita, I. Nakanishi, K. Kitaura, A. Hirasawa, G. Tsujimoto, T. Tada, *Bioorg. Med. Chem. Lett.* **2009**, *19*, 2920–2923.
- [19] A. Chilin, R. Battistutta, A. Bortolato, G. Cozza, S. Zanatta, G. Poletto, M. Mazzorana, G. Zagotto, E. Uriarte, A. Guiotto, L. A. Pinna, F. Meggio, S. Moro, *J. Med. Chem.* **2008**, *51*, 752–759.
- [20] M. Sharma, L. Li, J. Cerver, C. Killian, A. Koor, N. P. Seeram, *J. Agric. Food Chem.* **2010**, *58*, 3965–3969.
- [21] M. Larrosa, A. Gonzalez-Sarrias, M. J. Yanez-Gascon, M. V. Selma, M. Azorin-Ortuno, S. Toti, F. Tomas-Barberan, P. Dolara, J. C. Espin, *J. Nutr. Biochem.* **2010**, *21*, 717–725.
- [22] N. P. Seeram, Y. Zhang, R. McKeever, S. M. Henning, R. P. Lee, M. A. Suchard, Z. Li, S. Chen, G. Thames, A. Zerlin, M. Nguyen, D. Wang, M. Dreher, D. Heber, *J. Med. Food* **2008**, *11*, 390–394.
- [23] J. S. Duncan, D. W. Litchfield, *Biochim. Biophys. Acta Proteins Proteomics* **2008**, *1784*, 33–47.
- [24] N. A. St-Denis, D. W. Litchfield, *Cell Mol. Life Sci.* **2009**, *66*, 1817–1829.
- [25] G. Di Maira, M. Salvi, G. Arrigoni, O. Marin, S. Sarno, F. Brustolon, L. A. Pinna, M. Ruzzene, *Cell Death Differ.* **2005**, *12*, 668–677.
- [26] G. Di Maira, F. Brustolon, L. A. Pinna, M. Ruzzene, *Cell Mol. Life Sci.* **2009**, *66*, 3363–3373.
- [27] D. Ponce, J. L. Maturana, P. Cabello, R. Yefi, I. Niechi, E. Silva, R. Armisen, M. Galindo, M. Antonelli, J. C. Tapia, *J. Cell. Physiol.* **2010**, *226*, 1953–1959.
- [28] J. W. Cheong, Y. H. Min, J. I. Eom, S. J. Kim, H. K. Jeung, J. S. Kim, *Anti-cancer Res.* **2010**, *30*, 4625–4634.
- [29] M. Koronkiewicz, M. Zukowska, Z. Chilmonczyk, A. Orzeszko, Z. Kazmierczak, *Acta Pol. Pharm.* **2010**, *67*, 635–641.
- [30] A. Siddiqui-Jain, D. Drygin, N. Streiner, P. Chua, F. Pierre, S. E. O'Brien, J. Bliesath, M. Omori, N. Huser, C. Ho, C. Proffitt, M. K. Schwaeb, D. M. Ryckman, W. G. Rice, K. Anderes, *Cancer Res.* **2010**, *70*, 10288–10298.
- [31] S. Shahrzad, I. Bitsch, *J. Chromatogr. A* **1996**, *741*, 223–231.
- [32] B. S. Dhingra, A. Davis, *J. Chromatogr.* **1988**, *447*, 284–286.
- [33] J. Pandey, A. K. Jha, K. Hajela, *Bioorg. Med. Chem.* **2004**, *12*, 2239–2249.
- [34] F. Meggio, A. D. Deana, L. A. Pinna, *J. Biol. Chem.* **1981**, *256*, 11958–11961.
- [35] S. Sarno, P. Vaglio, F. Meggio, O. G. Issinger, L. A. Pinna, *J. Biol. Chem.* **1996**, *271*, 10595–10601.
- [36] J. Bain, L. Plater, M. Elliott, N. Shpiro, C. J. Hastie, H. McLaughlan, I. Klevernic, J. S. Arthur, D. R. Alessi, P. Cohen, *Biochem. J.* **2007**, *408*, 297–315.
- [37] Y. Cheng, W. H. Prusoff, *Biochem. Pharmacol.* **1973**, *22*, 3099–3108.
- [38] MOE-Dock, Molecular Operating Environment (MOE 2009.10), The Chemical Computing Group, Montreal, Canada; Homepage: <http://www.chemcomp.com> (Last accessed: September 26, 2011).
- [39] GOLD suite (version 5.1), The Cambridge Crystallographic Data Centre (CCDC), Cambridge, UK, **2011**; Homepage: www.ccdc.cam.ac.uk/products/life_sciences/gold/ (Last accessed: August 23, 2011).
- [40] R. A. Friesner, J. L. Banks, R. B. Murphy, T. A. Halgren, J. J. Klicic, D. T. Mainz, M. P. Repasky, E. H. Knoll, M. Shelley, J. K. Perry, D. E. Shaw, P. Francis, P. S. Shenkin, *J. Med. Chem.* **2004**, *47*, 1739–1749.

Received: July 11, 2011

Revised: August 12, 2011

Published online on October 4, 2011